Search for Right Handed Coupling in ν-N Scattering

S. R. Mishra,[a] W. C. Leung, C. Arroyo, K. T. Bachmann,[b] R. E. Blair,[c] C. Foudas,[d] B. J. King, W. C. Lefmann, E. Oltman,[e] P. Z. Quintas, S. A. Rabinowitz, F. J. Sciulli, W. G. Seligman, and M. H. Shaevitz
Columbia University, New York, New York 10027

F. S. Merritt, M. J. Oreglia, and B. A. Schumm[d]
University of Chicago, Chicago, Illinois 60637

R. H. Bernstein, F. Borcherding, H. E. Fisk, M. J. Lamm, W. Marsh, K. W. B. Merritt, H. Schellman, and D. D. Yovanovitch
Fermilab, Batavia, Illinois 60510

A. Bodek, H. S. Budd, P. de Barbaro, and W. K. Sakumoto
University of Rochester, Rochester, New York 14627

P. H. Sandler and W. H. Smith
University of Wisconsin, Madison, Wisconsin 53706
(Received 2 December 1991)

The relative absence of $\bar{\nu}_\mu$-induced charged current events with respect to ν_μ-induced events at large x (>0.45) and large y (>0.70) enables us to limit the right handed coupling of the weak current. Our data restrict $|\eta|^2=|g_R/g_L|^2<0.0015$ with 90% C.L. Within the framework of left-right symmetric models, this measurement imposes a limit upon the mixing angle of the left and right handed bosons. Unlike the limits imposed by the μ-decay and nuclear β-decay experiments, our limit is valid irrespective of the mass of the right handed neutrino.

PACS numbers: 13.15.Dk, 12.15.Cc

The y dependence of the differential cross section of neutrino interactions reflects the helicity of the weak current. If there were right handed coupling, the ν_μ-N and $\bar{\nu}_\mu$-N differential cross sections would assume forms

$$\frac{d\sigma^\nu}{dx\,dy}=\frac{G^2ME_\nu}{\pi}\{[q(x)+(1-y)^2\bar{q}(x)]+|\eta|^2[\bar{q}(x)+(1-y)^2q(x)]\}\,, \quad (1a)$$

$$\frac{d\sigma^{\bar{\nu}}}{dx\,dy}=\frac{G^2ME_\nu}{\pi}\{[\bar{q}(x)+(1-y)^2q(x)]+|\eta|^2[q(x)+(1-y)^2\bar{q}(x)]\}\,, \quad (1b)$$

where the parameter $|\eta|=|g_R/g_L|$ signifies the relative coupling of the right and left handed currents. We assume a left (right) handed ν_μ ($\bar{\nu}_\mu$), created in π^+ or K^+ (π^- or K^-) decay, interacting via a $V-A$ current at the lepton vertex; the right handed coupling evinces at the quark vertex (see below). Theories with manifest left-right symmetry make a definite prediction about $|\eta|$ in ν-N scattering [1]. In such theories, with the enlarged gauge group, $SU(2)_L\times SU(2)_R\times U(1)$, left ($W_L$) and right ($W_R$) handed bosons mix:

$$W_1=W_L\cos\zeta+W_R\sin\zeta\,,\qquad W_2=-W_L\sin\zeta+W_R\cos\zeta\,. \quad (2)$$

The left handed currents couple predominantly to W_1 and the right handed to W_2. The left (g_L) and the right (g_R) handed coupling in these models are $g_L=(\cos^2\zeta)/M_1^2+(\sin^2\zeta)/M_2^2$ and $g_R=\sin\zeta\cos\zeta(1/M_1^2-1/M_2^2)$, where M_1 (M_2) is the mass of W_1 (W_2). The parameter $|\eta|$, whose nonzero value indicates the existence of right handed coupling, is then expressed as $|\eta|=|g_R/g_L|=\zeta(1-M_1^2/M_2^2)=\zeta(1-\epsilon)$.

The parameter $|\eta|$ is measured by forming the ratio of two structure functions: $q_L(x)=q(x)+|\eta|^2\bar{q}(x)$ and $q_R(x)=\bar{q}(x)+|\eta|^2q(x)$ in Eq. (1). Structure functions q_L and q_R are extracted from the y dependence of the differential cross sections in Eq. (1). For large values of y, where the terms of the order $(1-y)^4$ become negligible, $q_R(x)$ can be expressed as

$$q_R(x)\propto\frac{d\sigma^{\bar{\nu}}}{dx\,dy}-(1-y)^2\frac{d\sigma^\nu}{dx\,dy}\,. \quad (3)$$

Experimentally, for large values of x, $q_R(x)\ll q_L(x)$. This imposes an upper limit on the sum $\bar{q}(x)+|\eta|^2q(x)$. Limits on the right handed coupling in ν-N scattering have been obtained by the CERN-Dortmund-Heidelberg-Saclay Collaboration [2]. Here, in a similar analysis, we present a more accurate measurement of $|\eta|^2$ at an average $Q^2=170$ GeV^2, and with neutrino energies extending up to 600 GeV.

Neutrino data were accumulated using the Fermilab Tevatron quadrupole triplet neutrino beam (QTB) with the Columbia-Chicago-Fermilab-Rochester (CCFR) de-

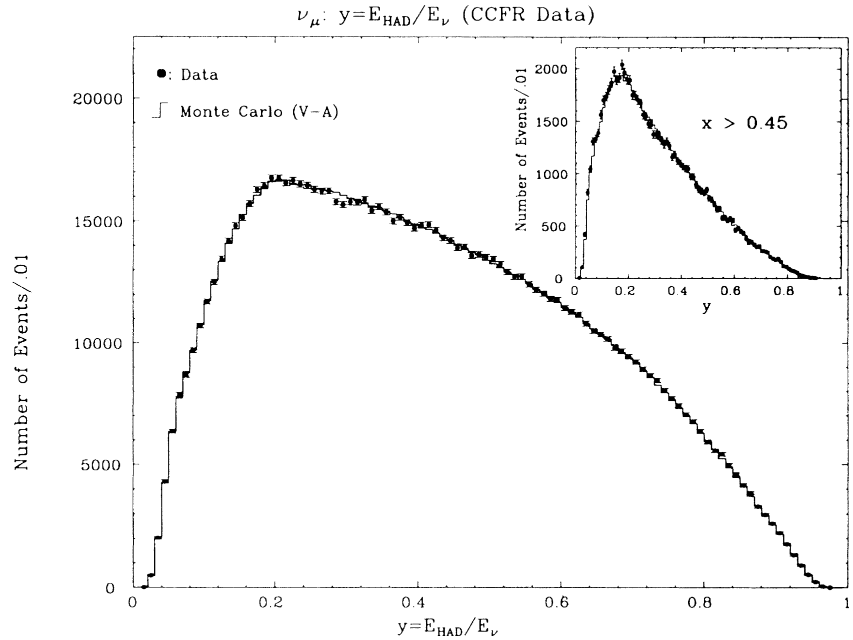

FIG. 1. Distribution of the variable $y=E_{\rm HAD}/E_\nu$ for ν_μ-induced charged current events after imposing cuts on muon momentum and hadron energy. The $V-A$ Monte Carlo prediction is shown as a histogram. Inset: The y distribution for events with $x>0.45$.

tector [3]. The QTB contained muon neutrinos and antineutrinos in the ratio $\simeq 2/1$ with usable neutrino energy in the range $10\le E_\nu \le 600$ GeV ($\langle E_\nu\rangle = 160$ GeV). The CCFR detector consists of a target calorimeter instrumented with scintillation counters and drift chambers, followed by a toroidal muon spectrometer. The initial sample of 3.7×10^6 muon triggers was required to have a transverse position of the interaction vertex within a square of 2.54 m×2.54 m centered in the target calorimeter, position of the vertex along the beam direction at least 4.4 m upstream of the downstream end of the 16.8 m long target, and a muon track in the spectrometer. The muon track was required to have an energy $E_\mu \ge 9$ GeV, and an angle $\theta_\mu \le 250$ mrad. The surviving sample of events with one muon consisted of 1.8×10^6 ν_μ- and 3.6×10^5 $\bar\nu_\mu$-induced events. For the structure function

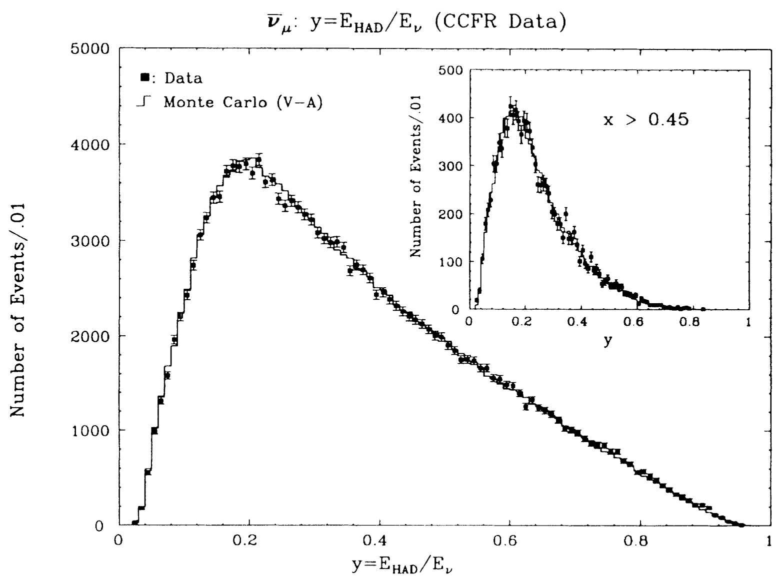

FIG. 2. Distribution of the variable $y=E_{\rm HAD}/E_\nu$ for $\bar\nu_\mu$-induced charged current events after imposing cuts on muon momentum and hadron energy. The $V-A$ Monte Carlo prediction is shown as a histogram. Inset: The y distribution for events with $x>0.45$.

TABLE I. ν_μ and $\bar{\nu}_\mu$ events with large x,y: number of events, mean energy, and mean Q^2 for neutrinos and antineutrinos. The last column shows the Monte Carlo-corrected $|\eta|^2$.

		ν events			$\bar{\nu}$ events			
$x>$	$y>$	No.	E (GeV)	Q^2 (GeV^2)	No.	E (GeV)	Q^2 (GeV^2)	$\lvert\eta\rvert^2$
0.45	0.70	5749	208	170	99	166	134	-0.00032 ± 0.00087
0.50	0.70	3459	215	188	63	176	152	-0.00010 ± 0.00112

analysis, an additional cut was imposed on the hadronic energy deposited in the calorimeter, $E_{\rm HAD}>10$ GeV.

Three empirical observations, in conjunction, obviate the need for a nonzero $|\eta|^2$. In Fig. 1 (Fig. 2) we present the observed ν_μ- ($\bar{\nu}_\mu$-) induced y distribution and compare it to the Monte Carlo prediction, which assumes a $V-A$ weak current. The comparison is shown in the entire x range, and in the $x>0.45$ range in the insets. The $V-A$ prediction describes the data well. Next, we show, in Fig. 3, $\bar{q}(x,Q^2)\approx 0.5[F_2(x,Q^2)-xF_3(x,Q^2)]$ in various x bins. The good agreement between the data and the Monte Carlo y distributions (Figs. 1 and 2), and the fact that $\bar{q}(x)$ is consistent with zero for $x\geq 0.45$ (Fig. 3), indicates that $|\eta|^2$ is consistent with zero within our experimental accuracy. Stated differently, these figures indicate that the ratio of antineutrino to neutrino cross sections at large and small values of x,

$$\left[\frac{d\sigma^{\bar{\nu}}}{dy}\Big/\frac{d\sigma^{\nu}}{dy}\right]_{x>0.45}\Big/\left[\frac{d\sigma^{\bar{\nu}}}{dy}\Big/\frac{d\sigma^{\nu}}{dy}\right]_{x<0.10},$$

is extremely small for large values of y. This observed small ratio, then, enables one to limit $|\eta|^2$.

Accordingly, on the sample of the ν_μ- and $\bar{\nu}_\mu$-induced charged current events, we imposed a cut $x>0.45$ and $y>0.70$. The resulting sample consisted of 5749 ν_μ- and 99 $\bar{\nu}_\mu$-induced events, respectively. The y distributions of ν_μ and $\bar{\nu}_\mu$ events with $x>0.45$ are shown in the insets of Figs. 1 and 2. The average energy and Q^2 of surviving events are 208 GeV and 170 GeV^2, respectively. We present these numbers in Table I along with numbers with a more stringent set of cuts ($x>0.50$, $y>0.70$). The upper limit on $|\eta|^2$ is obtained by extracting an upper limit on

$$\left[\frac{d\sigma^{\bar{\nu}}}{dx\,dy}-(1-y)^2\frac{d\sigma^{\nu}}{dx\,dy}\right]\Big/\left[\frac{d\sigma_{\nu}}{dx\,dy}-(1-y)^2\frac{d\sigma^{\bar{\nu}}}{dx\,dy}\right]. \quad (4)$$

Corrections due to geometric acceptance and resolution smearing were applied to the data using a Monte Carlo simulation. While forming the differential cross sections, terms involving factors of Q^2/ν^2 [not shown in Eq. (1)] were retained, and are included in the final answer. In addition, model corrections due to radiative, isoscalar, charm quark threshold, and propagator effects were incorporated. The effect of a nonzero $R(\sigma_L/\sigma_T)$, neglected in Eq. (1) for clarity, was estimated in Monte Carlo studies using the alternative parametrization of $R_{\rm QCD}$, $R_{\rm QCD}$ with target mass effects, and $R_{\rm SLAC}$ [4]. The systematic uncertainties associated in the $|\eta|^2$ measurement are detailed in Table II. Our measurement for $|\eta|^2$ is

$$|\eta|^2(x<0.45,y>0.70)=-0.00032\pm0.00087\pm0.00026<0.0015\ (90\%\ \text{C.L.}). \quad (5)$$

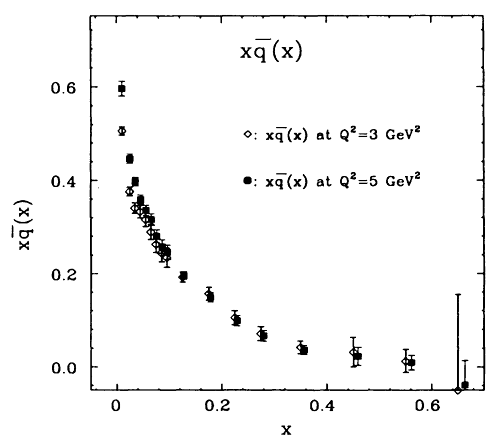

FIG. 3. The $\bar{q}(x)$ as a function of x at two $Q^2=3$ and 5 GeV^2.

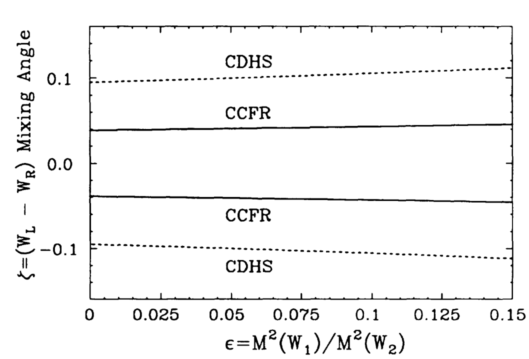

FIG. 4. Limits on the ζ-ϵ plane from neutrino experiments. These limits are independent of the mass of the right handed neutrino.

TABLE II. Systematic errors on $|\eta|^2$: estimates of systematic errors on $|\eta|^2$ due to radiative correction, relative flux determination, and R parameter.

Sources	$\pm\delta|\eta|^2$
Radiative correction	0.00004
Relative flux ($\pm 2\%$)	0.00017
R	0.00020

As mentioned earlier, theories with manifest left-right symmetry are constrained by our measurement. Using the limit on $|\eta|^2$, we extract limits on the ζ-ϵ plane (see Fig. 4).

Precision measurements in μ-decay and nuclear β-decay experiments constrain regions in the ζ-ϵ plane (for details see Ref. [5]). These limits, however, apply to the special case when the right handed neutrino [corresponding to $SU(2)_R$] is light; typically the limits are applicable when $m_{\nu R} \lesssim 10$ MeV. Limits from our measurements, although competitive with those from muon experiments, are independent of this assumption.

We acknowledge the hospitality of the Fermilab staff and management, and the help given to us by many persons at our home universities. We thank the National Science Foundation and the U.S. Department of Energy for their support.

(a)Present address: Harvard University, Cambridge, MA 02138.
(b)Present address: Widener University, Chester, PA 19013.
(c)Present address: Argonne National Laboratory, Argonne, IL 60439.
(d)Present address: University of Wisconsin, Madison, WI 53706.
(e)Present address: Lawrence Berkeley Laboratory, Berkeley, CA 94720.

[1] M. B. A. Beg *et al.*, Phys. Rev. Lett. **38**, 1252 (1977); M. Gell-Mann, P. Ramond, and R. Slansky, Rev. Mod. Phys. **50**, 721 (1978).
[2] H. Abramowicz *et al.*, Z. Phys. C **12**, 225 (1982).
[3] S. R. Mishra *et al.*, Phys. Lett. B **252**, 170 (1990); also W. K. Sakumoto *et al.*, Nucl. Instrum. Methods Phys. Res., Sect. A **294**, 179 (1990).
[4] S. R. Mishra and F. Sciulli, Phys. Lett. B **244**, 341 (1990). SLAC measurements could be found in S. Dasu *et al.*, Phys. Rev. Lett. **61**, 1061 (1988). For the details of the empirical parametrization of the SLAC data see L. W. Whitlow, Ph.D. thesis (SLAC Report No. SLAC-357, 1990).
[5] M. Strovink, in *Proceedings of the Leptonic Session of the Twenty-First Recontre de Moriond, Les Arcs, March, 1986*, edited by J. Tran Thanh Van (Editions Frontieres, Gif-sur-Yvette, 1986), p. 209. See also A. Jodido *et al.*, Phys. Rev. D **34**, 1967 (1986).